Impact of 3D Clouds on Clear Sky Reflectance and Aerosol Retrieval in a Biomass Burning Region of Brazil

GUOYONG WEN[1,2]
ALEXANDER MARSHAK[1], AND ROBERT F. CAHALAN[1]

Short title: Cloud 3D and Aerosols

IEEE, Geoscience Remote Sensing Letters

(Accepted, 2005)

[1] NASA Goddard Space Flight Center, Greenbelt, Maryland.
[2] Goddard Earth Sciences and Technology Center, U. of Maryland Baltimore County, Maryland.

Corresponding author address:
Guoyong Wen
NASA/GSFC, Code 613.2
Greenbelt, MD 20771

Authors - Dr. Guoyong Wen
Goddard Earth Sciences and Technology Center
University of Maryland Baltimore County
5523 Research Park Dr., Suite 320
Baltimore County, MD 21228
(301) 614-6220 (voice)
(301) 614-6307 (fax)
wen@climate.gsfc.nasa.gov

Dr. Alexander Marshak
NASA Goddard Space Flight Center
Code 613.2
Greenbelt, MD 20771
(301) 614-6122

Dr. Robert F. Cahalan
NASA Goddard Space Flight Center
Code 613.2
Greenbelt, MD 20771
(301) 614-5390

ABSTRACT

3D cloud radiative effects on clear sky reflectances and associated aerosol optical depth retrievals are quantified for a cumulus cloud field in a biomass burning region in Brazil through a Monte Carlo simulation. In this study the 1km MODerate-Resolution Imaging Spectroradiometer (MODIS) cloud optical depth and surface reflectance datasets are used to compute the 3D radiation fields with ambient aerosol optical thickness of 0.1 at a wavelength of 0.66 μm. The 3D radiative effects range from –0.015 to 0.018 with an average of 0.004 and standard deviation of 0.006. The 3D effects are most pronounced and variable for cloud neighboring pixels, where both large negative effects over shadows and positive effects near sunlit cloud edges are found. The clear next-to-cloud pixels, that contain ~83% of the clear pixel population, are affected in the most complex way and not reliable for aerosol retrieval. In the area 2 km away from clouds, the 3D effects enhance the reflectance in clear patches. The average and variability of enhancements gradually decrease as a function of the cloud-free distance, resulting in a systematically higher aerosol optical depth estimates for pixels closer to clouds in 1D retrieval. At a distance of 3 km away from clouds, the 3D effect is still appreciable with the average enhancement slightly less than 0.004. This enhancement will lead to an over estimate of aerosol optical thickness of ~0.04 in 1D retrieval, which is significant for an ambient atmosphere with aerosol optical thickness of 0.1.

1. INTRODUCTION

Since Twomey (1977) proposed the theory on the effect of aerosol on cloud properties, much research has been conducted to understand how aerosols modify clouds (e.g., Albrecht, 1989; Coakley et al., 1987; Kaufman and Fraser, 1997; Han et al., 1994; Feingold, 2003). Although more satellite data has become available to allow scientists to investigate aerosol-cloud interaction on a global scale, to quantify this interaction through satellite observations still remains a great challenge. To achieve this goal one needs to accurately determine both the ambient aerosol amounts and associated cloud properties. However, the large contrast between optically thin aerosols and optically thick clouds intramixed with each other makes it difficult to determine the aerosol amount with 1D retrievals because, in general, this is an essentially 3D problem.

In the past few years, efforts have been made to quantify 3D radiative effects of clouds on the aerosol retrieval in nearby cloud-free region. For example, 3D radiative effects of clouds on reflected sunlight have been observed from Landsat images (Cahalan *et al.*, 2001; Wen *et al.*, 2001), and a parameterization method was proposed to quantify such effects (Wen *et al.*, 2001). Extensive 3D Monte Carlo simulations were performed for cuboidal bar and cubic shaped clouds to estimate the effects of clouds on surface reflectance and aerosol retrievals from satellite observations (Kobayashi *et al.*, 2000; Cahalan *et al.*, 2001).

This paper is an extension of our previous research. In contrast to earlier 3D modeling studies, this work is based on a realistic cumulus cloud field in a biomass burning region in Brazil. State-of-the-art 3D Monte Carlo (MC) radiative transfer models (Marshak and Davis, 2005; Cahalan *et al.*, 2005) make it possible to accurately compute the radiation fields in complex cloudy atmospheric conditions. In this paper, optical properties of cloud field, aerosols and surfaces for the 3D computation are described in section 2. Section 3 provides the results of the study followed by a summary and discussion of the results in the final section.

2. CLOUD, AEROSOL AND SURFACE PROPERTIES

Fig. 1 shows a 1 km resolution cloud optical depth image retrieved from MODerate-Resolution Imaging Spectroradiometer (MODIS) observations (Platnick *et al.*, 2003). The image is centered on the equator at 53.78 degrees West and was taken on January 25, 2003 with solar zenith angle of 32 degrees and solar azimuth angle of 129 degrees and nadir viewing geometry. The domain of the simulation is 80 x 68 at 1 km resolution, which completely covers an Advanced Spaceborne Thermal Emission and Reflection Radiometer (ASTER) image of size ~60 km x 60 km (Yamaguchi *et al.*, 1998). The

cloud cover is 53 percent. The phase function at 0.66 μm is computed assuming a gamma distribution of cloud droplet with effective radius of 10 μm and effective variance of 0.1 (Hansen, 1971). The cloud top height is determined from the brightness temperature at 11 μm from MODIS channel 31, and the cloud base is assumed constant at 1km. We also assume a linear vertical profile of cloud liquid water. The case is chosen for the increasing interest in cloud aerosol interaction research in the biomass burning region (e.g., Andreae *et al.*, 2004), and was selected as a phase 3 case for the I3RC (Cahalan *et al.*, 2005). This scene is also typical for fair weather cumulus, as discussed in section 3.

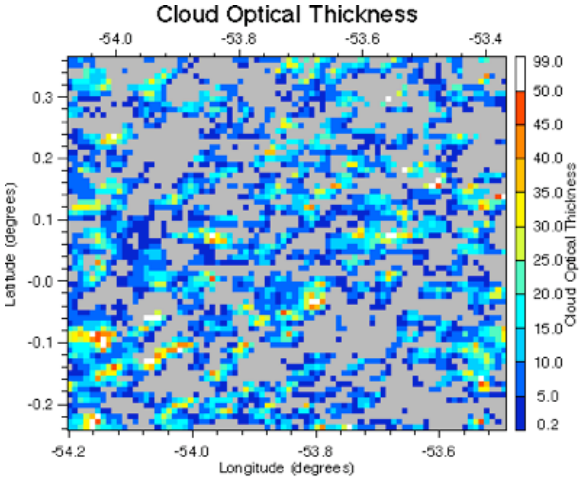

Figure 1. Cloud optical thickness field from MODIS retrievals.

The aerosol is assumed to have a lognormal size distribution with log of standard deviation of 0.7 and effective radius of 0.13 μm. The single scattering albedo is 0.93. The aerosol amount with optical thickness of 0.1 is assumed to be uniformly distributed in two layers, with the lower troposphere below 2 km and the free troposphere above. The aerosol optical thickness in the free troposphere is assumed to be 0.01 with remaining aerosols in the lower troposphere. Rayleigh scattering is also taken into account.

The value-added surface datasets derived from MODIS land products (Moody et al., 2005) show that the surface in the region is covered by vegetation: it is dark and homogeneous in the visible wavelength at 0.66 μm. The average white-sky and black-sky albedos (Moody et al., 2005) in the region are 0.025 and 0.021 with standard deviations of 0.004 and 0.003 respectively. For simplicity, a Lambertian surface with albedo of 0.023 is used as a lower boundary condition.

3. 3D RADIATIVE EFFECTS

A 3D MC scheme (Marshak and Davis, 2005; Cahalan *et al.*, 2005) is used to compute the nadir reflectance at 0.66 μm for cloud, atmospheric optical, surface properties, and sunangle as described in section 2. Since the 3D radiative effects of clouds on clear region reflectances are the primary interest in this study, we compare the "true" reflectance fields from a full 3D simulation with its 1D counterpart only for clear pixels. The 3D radiative effect of cloud is defined as $r_{3D} - r_{1D}$, where r_{3D} is the "true" reflectance of a clear pixel in the cumulus field calculated using a full 3D simulation while r_{1D} is its 1D counterpart. For cloud free atmosphere, the reflectance is $r_{1D} = 0.0435$.

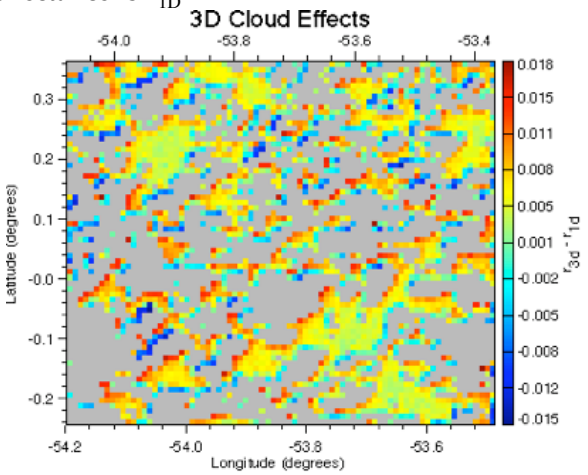

Figure 2. 3D radiative effects of cloud on reflectance of clear pixels with the direction of incident solar radiation indicated. Cloudy pixels are in gray.

The 3D cloud effects at pixel level are presented in Fig. 2. The clouds are indicated as gray. It is evident that cumulus clouds could either reduce (negative effect) or enhance (positive effect) the clear region reflectance with the 3D effects ranging from -0.015 to 0.018. There are two important features immediately identified from Fig. 2. First, clouds cast shadows on the ground leading to large reductions of reflectance over shadowed pixels. Second, clouds enhance clear region reflectance everywhere else. The largest enhancements are found for clear pixels adjacent to the sunlit side

of clouds. The overall and detailed statistics of the enhancement are described below.

Fig. 3 shows the cumulative distribution of 3D effects for all clear pixels. The average 3D effect is about 0.004 with standard deviation about 0.006. The distribution of the 3D effects is asymmetric indicating different origins in the population of the distribution. The long tail of negative 3D effects extending to –0.015 comes from shadowed pixels, while the large value of 3D effects at the end of the positive tail comes from pixels adjacent to the sunlit side of clouds as explained in detailed analysis below.

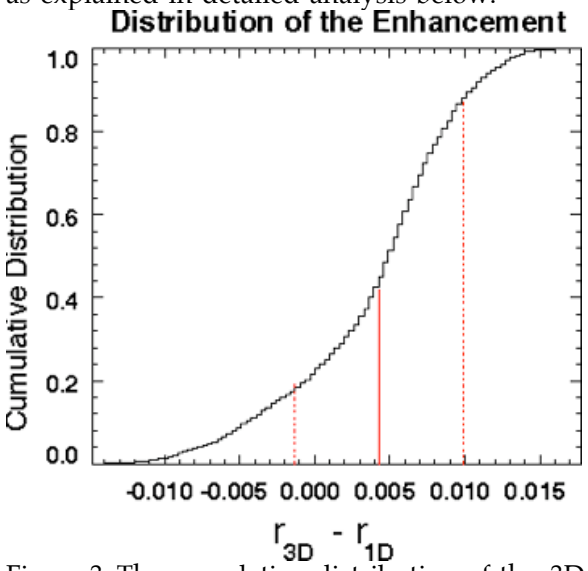

Figure 3. The cumulative distribution of the 3D effect with the average (~0.0043) indicated by the solid line, and one standard deviation (~0.0056) from the average indicated by the dotted lines. The cloud free 1D reflectance is 0.0435.

It is interesting to examine the statistics of reflectance for pixels with the same distance away from the nearest cloud. The nearest cloud distance of a clear pixel is defined as the distance from the center of that pixel to the center of the nearest cloudy pixel. In a discrete grid field, the nearest cloud distance (d) is calculated from the difference in rows (Δi) and columns (Δj) between the clear and cloud pixels and the grid size ds, i.e., $d = \sqrt{\Delta i^2 + \Delta j^2}\,ds$. For a grid size of 1 km only a discrete set $(d_1, d_2, d_3, d_4, d_5, ...)$ or $(1, \sqrt{2}, \sqrt{5}, 2\sqrt{2}, 3, ...)$(km) of nearest cloud distance is allowed. The nearest cloud distance not only gives a measure of the distance between a clear pixel and the nearest cloudy pixel, but also determines the range of a completely clear area from that clear pixel. For a given clear pixel with the nearest cloud distance of d_k, the area with a radius of d_{k-1} around this pixel is completely clear.

Fig. 4 shows the statistics of the enhancement for clear pixels with different nearest cloud distances. It is apparent that the reflectance statistics (circles) falls into two categories. The first one ($d < 2$km) is classified as "cloud neighboring region", and the second one ($d \geq 2$km) as "open area". In the cloud neighboring region, the reflectance is largely enhanced or reduced for clear pixels depending on sunlit or shadowed side of clouds. This results in a large variability in the 3D effects. The variabilities of the 3D effect as measured by the standard deviation are 0.006 and 0.004 for pixels next to clouds ($d = 1$km) and pixels diagonally next to clouds ($d = \sqrt{2}$km) respectively. Since the variability in the 3D effect is so large, the cloud neighboring pixels are absolutely not reliable for aerosol retrieval.

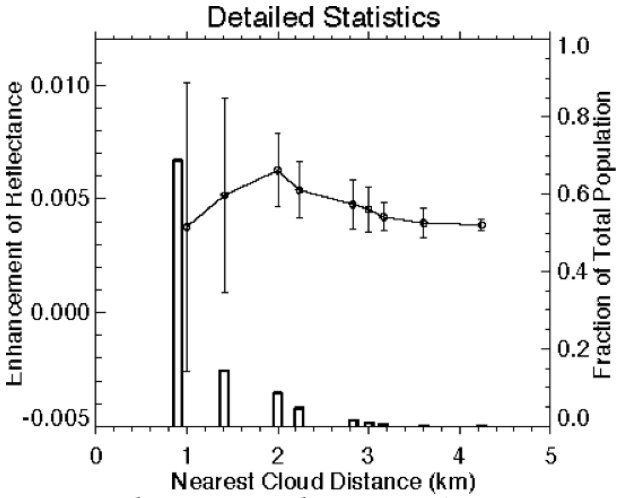

Figure 4. The average enhancement (circles, left scale) and standard deviation (vertical brackets) for clear pixels with different nearest cloud distance . Vertical bars show the fraction of clear pixels (right scale) as a function of the nearest cloud distance. The first bar at 1km nearest cloud distance is shifted slightly for clarity. The total number of clear pixels is 2541. The cloud free 1D reflectance is 0.0435.

The average 3D effect in the cloud neighboring region is a result of a competition between shadowing reduction and diffuse enhancement. For a dark surface with 0.023

surface albedo, the average 3D effect is positive. Moving away from clouds, the diffuse enhancement dominates and the average enhancement of reflectance increases, reaching a maximum about 0.006 at nearest cloud distance of 2 km, then decreases monotonically. The increase in the average of the enhancement within the cloud neighboring region is primarily due to the fact that the ratio of shadowing pixels to the total pixels decreases with the distance as shadowing diminishes and as one moves farther away from clouds, the number of negative extreme values decreases resulting in a decrease in the variability of the 3D effect.

In the open area with $d \geq 2\,\mathrm{km}$, both the average 3D effect and the associated variability decrease gradually as a function of nearest cloud distance, leading to a systematically higher 1D retrieval of aerosol optical thickness for clear pixels closer to clouds. At a distance of 3 km away from clouds, the average enhancement reduces to 0.0045 with a standard deviation of 0.001. However the enhancement does not decrease to zero within the cloud field. Rather, the enhancement reaches an appreciable value slightly less than 0.004. This enhancement will result in an over-estimate of AOD of 0.04 in 1D retrieval. The error is still significant for an atmosphere with true ambient aerosol optical thickness of 0.1.

Also, it should be noted that the cloud neighboring clear pixels contain 68.8% of the total clear pixel population of 2541 (Fig. 4). This fraction will be 83.2% if clear pixels diagonally next to a cloud are included. With strong variability in the 3D effects, this large amount of cloud neighboring pixels appears not reliable in simple 1D retrieval. Away from clouds, the clear pixel population drops rapidly. The clear pixel population falls to less than 2% of the total population for $d \geq 3\,\mathrm{km}$. The distribution resembles cloud spacing distributions both from satellite and ground based observations (i.e., Fig. 2. of Joseph and Cahalan, 1990; Figs.6,7 of Lane et al., 2002), and is probably typical for fair weather cumulus. Such rapid decrease in clear pixel population away from cloud in a fair weather cumulus region is an obstacle for any efforts to use clear pixels far away from clouds for retrieval of aerosol optical properties.

4. SUMMARY AND DISCUSSIONS

3D radiative effects on clear region reflectance and aerosol retrievals are quantified for a realistic cumulus cloud field over a dark surface with Lambertian albedo of 0.023 over a biomass burning region in Brazil. The results show that clouds cast shadows to reduce the reflected sunlight and enhance reflectance almost everywhere else in clear patches in cumulus cloud fields. The 3D effect ranges from –0.015 to 0.018 with an average of 0.004 and standard deviation of 0.006 for all clear pixels. The relatively small average effect is primarily due to the diffusive enhancement compensated by relatively large shadowing reduction in the domain average.

Detailed analyses show that the reduction of reflectance occurs over cloud shadows. Large enhancement in reflectance is found for pixels next to the sunlit side of clouds. The average enhancement of clear region reflectance increases as a function of the nearest cloud distance reaching a maximum at the nearest cloud distance of 2 km, and decreases monotonically. Within the cloud neighboring region, the increase in the average enhancement away from clouds is primarily due to a decrease in the ratio of shadowed pixels to the total number of pixels as a function of the distance from clouds, and a much larger shadowing reduction effect than diffuse enhancement effect. Cloud neighboring pixels, including those diagonally next to clouds, which contain ~83% of all clear pixel population, are affected in a complex way, with large variability in 3D effect. Therefore, cloud neighboring pixels are not reliable for aerosol retrieval.

In the open area, the enhancement of reflectance and associated variability decrease gradually as a function of nearest cloud distance resulting in systematically higher 1D aerosol optical thickness retrieval for pixels closer to clouds. As the distance to the nearest cloud increases, the clear pixel population drops rapidly adding additional difficulties in aerosol retrieval. The population of clear pixels with nearest cloud distance $d \geq 3\,\mathrm{km}$ drops to less than 2% of the total clear pixel population. It should be noted that clear pixels at a distance of 3 km away from clouds are still affected by clouds with the enhancement slightly less than 0.004. This enhancement corresponds to an over-estimate of aerosol

optical depth of 0.04 in 1D retrieval which is still significant for an atmosphere with ambient aerosol optical depth of 0.1.

One should notice that 3D effects of real fair weather cumulus are appreciably different from those of a simple shaped isolated optically thick cloud. First, the open space in a fair weather cumulus is rather limited to a range of less than 4 km. Second, at a distance 4km away from clouds in the clear region, the fair weather cumulus imposes larger effects on clear region reflectance with enhancement of ~0.004 for fair weather cumulus vs. enhancement ~0.002 for a single optically thick cloud (e.g., Fig. 11 of Cahalan et al., 2001). The larger enhancement about 0.004 is consistent with the enhancement in path radiance at both red and blue bands observed from Landsat imagery (e.g., Fig. 8 in Wen et al., 2001). This discrepancy is primarily due to the fact that the open area is surrounded by puffy clouds in a realistic fair weather cumulus field, which effectively produces diffuse radiation, resulting in a higher enhancement in open area reflectance.

We also found that the vertical distribution of aerosols affects the enhancement. For the same amount of aerosols, the higher the altitude of aerosols, the larger the enhancement, and the smaller the shadowing reduction in clear region reflectance. One should notice that the aerosol is assumed horizontally uniformly distributed in this study. In the real world, aerosol properties in the vicinity of clouds may vary, making for even more complicated aerosol retrieval. The magnitude of 3D effects also depends on solar zenith angle as discussed by Nikolaeva *et al.* (2005).

Finally, we conclude that 3D radiative effects of cloud are important in quantifying ambient aerosol amount in a cumulus cloud field. Furthermore, special caution must be made in applying 1D techniques or using 1D retrieved aerosol data in aerosol-cloud interaction research.

Acknowledgments. This research was supported by funding provided by NASA and DoE's ARM program.

REFERENCES

Andreae, M. O., D. Rosenfeld, P. Artaxo, A.A. Costa, G.P. Frank, K.M Longo, M.A.F. Silva-Dias, Samoking Rain Clouds over the Amazon, *Science* 27 February 2004; 303: 1337-1342 , DOI: 10.1126/science.1092779.

Cahalan, R.F., and 35 coauthors, The International Intercomparison of 3D Radiation Codes (I3RC), bring together the most advanced radiative transfer tools for cloud atmospheres, *Bulletin of American Meteorological Society, Accepted, 2005.*

Coakley, J. A., Jr., R. L. Bernstein, and P. A. Durkee, Effect of ship-track effluents on cloud reflectivity, *Science*, 237, 1020-1022, 1987.

Feingold, G., Modeling of the first indirect effects: Analysis of measurement requirements, *Geophy. Res. Lett.*, *30*(19), 1997, doi:10.1029/2003GL017967, 2003.

Han, Q., W. Rossow, and A. Lacis, Near-global survey of effective droplet radii in liquid water cloud using ISCCP data, *Journal of Climate*, 7, 465-497, 1994.

Hansen, J., Multiple scattering of polarized light in planetary atmospheres. Part II. Sunlight reflected by terrestrial water clouds, *J. Atmos. Sci., 28*, 1400-1426, 1971.

Joseph, J.H. and R.F. Cahalan, Nearest Neighbor Spacing of Fair Weather Cumulus Clouds, *J. Appl., Meteor., 29*, 793-805, 1990.

Kaufman, Y., and R. Fraser, The effect of smoke particles on clouds and climate forcing, *Science*, 277, 1636-1639, 1997.

Kaufman, Y., and 11 other coauthors, A critical examination of the residual cloud contamination and diurnal sampling effects on MODIS estimates of aerosol over ocean, *IEEE Trans. Geosci. Remote Sensing*, accepted, 2005.

Lane D.E., K. Goris, and R.C.J. Somerville, Radiative Transfer through Broken Clouds: Observations and Model Validation, *J. Climate., 15*, 2921-2933, 2002.

Marshak, A. and A. Davis, *3D Radiative Transfer in Cloudy Atmospheres*, Springer. 2005.

Moody, E. G., M. D. King, S. Platnick, C. B. Schaaf, and F. Gao, Spatially complete global spectral surface albedos: Value-Added datasets derived from Terra MODIS land products. *IEEE Trans. Geosci. Remote Sens.*, **43**, 144-158, 2005.

Nikolaeva O. V., L.P. Bass, T.A. Germogenova, A.A. Kokhanovisky, V.S. Kuznetsov, B. Mayer, The influence of neighboring clouds on the clear sky reflectance with the 3-D

transport code RADUGA. *J. Quant. Spectros. Radiat. Transfer.*, **94**, 405-424, 2005.

Platnick, S., M. King, S. Ackerman, W. P. Menzel, B. Baum, J. C. Riedi, and R. A. Frey, The MODIS cloud products: algorithms and examples from Terra, *IEEE Trans. Geosci. Remote Sensing*, vol 41, 459-473, 2003.

Remer, L., and 12 other coauthors, The MODIS Aerosol Aolgorithm, Products, and Validation, *J. Atmos. Sci. Speccial Section*, vol 62, 947-973, 2005.

Twomey, S., The influence of pollution on the shortwave albedo of clouds, *J. Atmos. Sci.*, vol 34, 1149-1152, 1977.

Yamaguchi, Y., A. B. Kahle, H. Tsu, T. Kawakami, and M. Pniel, Overview of Advanced Spaceborne Thermal Emission and Reflection Radiometer (ASTER), *IEEE Trans. Geosci. Remote Sensing*, vol 36, 1062-1071, 1998.

Wen, G., R. F. Cahalan, S-C Tsay, and L. Oreopoulos, Impact of cumulus cloud spacingon Landsat atmospheric correction and aerosol retrieval, *J. Geophys. Res.*, 106, 12,129-12,138, 2001.